JOURNAL OF MATERIALS SCIENCE 7 (1972) 1265–1279

The energy of crack propagation in carbon fibre-reinforced resin systems

PETER W. R. BEAUMONT*, BRYAN HARRIS
Materials Science Division, School of Applied Sciences, University of Sussex, Brighton, UK

The energy expended during controlled crack propagation in unidirectionally reinforced composites of carbon fibre in a brittle resin matrix has been evaluated in terms of the energy dissipated during fibre-snapping, matrix-cracking and fibre pull-out. The work of fracture, γ_F, is found to depend principally on the frictional shear stress at the fibre/resin interface opposing pulling out of broken fibres. Differences in γ_F for carbon fibre/resin composites exhibiting a range of interfacial shear strengths and void contents have been explained with reference to variations in fracture surface topography of the fibrous composites. The effect of environment on properties of the interface and work of fracture was also investigated. The energy required to propagate a crack has been compared with the energy for fracture initiation, γ_I, using a linear elastic fracture mechanics approach. It was found that fibre pull-out energy is the principal contribution to γ_F, and γ_I is similar to the elastic strain energy release rate at the initiation of fracture of a brittle, orthotropic solid. For crack propagation *parallel* to fibres, γ_F and γ_I are similar and not unlike the fracture surface energy of the resin alone. The strength of the interface is important only in so far as it affects the value of γ_I.

1. Introduction

An understanding of the events leading to initiation and growth of microcracks in composite materials under the combined action of stress and some active environment should indicate the important parameters for the design of a tough, notch-insensitive engineering material. Although the prevention of flaws and voids in materials is highly desirable, their presence is nevertheless an inherent feature of some types of composite. Quite apart from the existence of internal flaws in fibres, it is not unusual to find interfacial or matrix porosity in the form of pockets of air trapped during the fabrication process. This raises the question of how composites containing these and worse imperfections, such as cracks, will perform under load, particularly in the presence of an environment other than air.

The experiments described here have been carried out from a fracture mechanics viewpoint. We have measured the work required to fracture unidirectionally reinforced composites of carbon fibre in epoxy resin (CFRP) perpendicular to and parallel with the fibre direction, using both sound and porous materials. We have attempted to establish the nature of the major energy absorbing fracture processes in CFRP and to isolate the mechanisms which influence crack motion. The effect of moisture and oil on fracture mechanisms has also been investigated.

2. A fracture mechanics approach to the failure of fibrous composites

The resistance of a solid to microcracking, leading to the formation of macrocracks, can be evaluated quantitatively by determining the fracture "surface' energy of the solid. In isotropic materials, the release of stored elastic strain energy per unit area of fracture surface during initiation of microcracking, γ_I, may be similar to the energy dissipated during its extension to macrocrack dimensions, leading to ultimate failure of the material. The relationship between γ_I and the ultimate strength of the cracked solid, σ_f, is described by the classical equation given by Griffith [1]:

$$\gamma_I = \frac{\sigma_f^2 (\pi c)}{2E} \quad (1)$$

*Now at the School of Engineering and Applied Sciences, University of California, Los Angeles, California, USA.

where c is the critical size of flaw, and E is the Young's modulus of the solid.*

In composite materials, the multiplicity of microfracture processes which influence the formation and growth of microcracks makes the separation of their characteristic energy-release rates extremely difficult. The mechanism controlling the slow growth of a crack may be quite different from that influencing its rapid propagation and, as a consequence, the resistance of the composite to crack nucleation may not be the same as for growing cracks [2].

The fracture surface energy of a carbon fibre-reinforced polyester resin is much greater than the sum of the fracture surface energy of the fibre, γ_f, and resin matrix, γ_m [3]. Additional energy must, therefore, be absorbed by other microfracture processes as the crack extends through the composite. Fracture mechanisms that have been proposed to account for this extra energy include: (1) relaxation of a fibre when it snaps, γ_r [4]; (2) debonding energy released during separation of fibre and resin, γ_d [5]; and (3) fibre pull-out energy, γ_p, to overcome friction at the fibre/resin interface, during extraction of the fibre [6]. The total work to fracture the composite, γ_c, is now considered as the sum of these fracture energies:

$$\gamma_c = \gamma_f + \gamma_m + \gamma_r + \gamma_d + \gamma_p$$

However, one or more of these microfracture processes may control different stages in the complete fracture of the composite, and the resistance of the composite to cracking will therefore vary as the crack extends.

Under certain conditions, the Griffith fracture concept may be applied to anisotropic materials and, by a further approximation, to the behaviour of fibrous composites. The problem of extending a crack in an *orthotropic* solid, has been considered by Sih, *et al* [7], and Wu [8]. Their calculations show that the usual Irwin-Westergaard expressions [9] describing the complete stress distribution about a crack tip must be modified by *functions containing the orthotropic elastic constants of the material*, but that the stress field intensities at the crack front are identical with those for an isotropic solid.

For an infinite plate containing a small crack, the stress intensification at the tip of the crack is given by:

$$K = \sigma_\infty \sqrt{(\pi c)} \qquad (2)$$

where K is the stress intensity factor and σ_∞ is the stress applied to the plate. When the crack reaches a critical size, K also becomes critical, K_c, and combining Equations 1 and 2:

$$K_c = \sqrt{(2E\gamma_I)} \qquad (3)$$

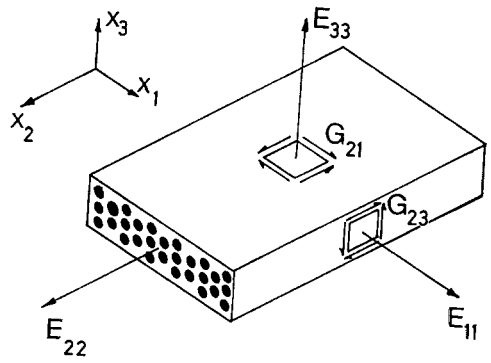

$$s_{11} = 1/E_{11} = 12.8 \times 10^{-2}\ (\mathrm{GNm^{-2}})^{-1}$$
$$s_{22} = 1/E_{22} = 0.68 \times 10^{-2}\ "$$
$$s_{12} = -\nu_{21}/E_{22} = -0.20 \times 10^{-2}\ "$$
$$s_{66} = 1/G_{21} = 36.2 \times 10^{2}\ "$$

Figure 1 Relationship between principal stress directions and fibre direction in composite.

If fracture is to occur on a plane of elastic symmetry (the x_1x_3 plane, Fig. 1) in a linear elastic orthotropic solid, the critical elastic strain energy-release rate for the opening fracture mode is:

$$G_{Ic} = K_{Ic}^2 \left[\frac{S_{11}S_{22}}{2}\right]^{\frac{1}{2}} \left[\left(\frac{S_{22}}{S_{11}}\right)^{\frac{1}{2}} + \left(\frac{2S_{12} + S_{66}}{2S_{11}}\right)\right]^{\frac{1}{2}} \qquad (4)$$

where S_{11}, S_{22}, etc., are the independent elastic compliances of the orthotropic solid for a thin plate in plane stress.

Rearranging Equation 4:

$$\frac{G_{Ic}}{K_{Ic}^2} = \frac{1}{E_{eff}} = \left[\frac{S_{11}S_{22}}{2}\right]^{\frac{1}{2}} \left[\left(\frac{S_{22}}{S_{11}}\right)^{\frac{1}{2}} + \left(\frac{2S_{12} + S_{66}}{2S_{11}}\right)\right]^{\frac{1}{2}} \qquad (5)$$

The reciprocal of the term on the right hand side of this equation can be considered as the "effective modulus" of the orthotropic solid for for crack propagation in the x_1x_3 plane. The S_{ij}

*In linear elastic fracture mechanics terminology $\gamma_I = G_{Ic}/2$: Equation 1 refers, of course, to a state of plane stress.

can be written in terms of the conventional engineering elastic moduli of the *composite*, as follows:

$$S_{11} = 1/E_{11}\ ; \quad S_{12} = -\nu_{12}/E_{11}$$
$$S_{22} = 1/E_{22}\ ; \quad S_{66} = 1/G_{12}$$

and E_{11}, E_{22}, ν_{12} and G_{12} can, in turn, be calculated from the known elastic properties of the *fibre and matrix* following an analysis by Tsai [10]. Using this analysis with the fibre and resin properties listed in Table I, and substituting the resulting values into Equation 6, we find that the composite effective modulus is approximately 38 GN m^{-2}.

TABLE I Fibre and resin elastic properties.

Engineering moduli	Carbon fibre	Epoxy resin
E_{22}	360 (GN m^{-2})	3.44 (GN m^{-2})
$E_{11} = E_{33}$	34.4 (GN m^{-2})*	3.44 (GN m^{-2})
$\nu_{21} \approx \nu_{23}$	0.2	0.35
G_{21}	34.4 (GN m^{-2})*	1.27 (GN m^{-2})

*Data from Tsai [10].

Thus if the critical stress intensity factor, K_{Ic}, can be measured experimentally, the critical elastic strain energy-release rate at the initiation of failure can be calculated using Equation 4. It is more useful to obtain values of γ_I than K_{Ic} since the critical energy-release rate will give some indication of the microfracture process controlling the formation of a microcrack. It is striking that the "effective" modulus is as low as one sixth of the normal value of E_{11} for the composite.

3. Experimental

3.1. Materials and fabrication

Epoxy resin plates reinforced with Morganite type I (high modulus) untreated and surface-treated carbon fibres were moulded using a

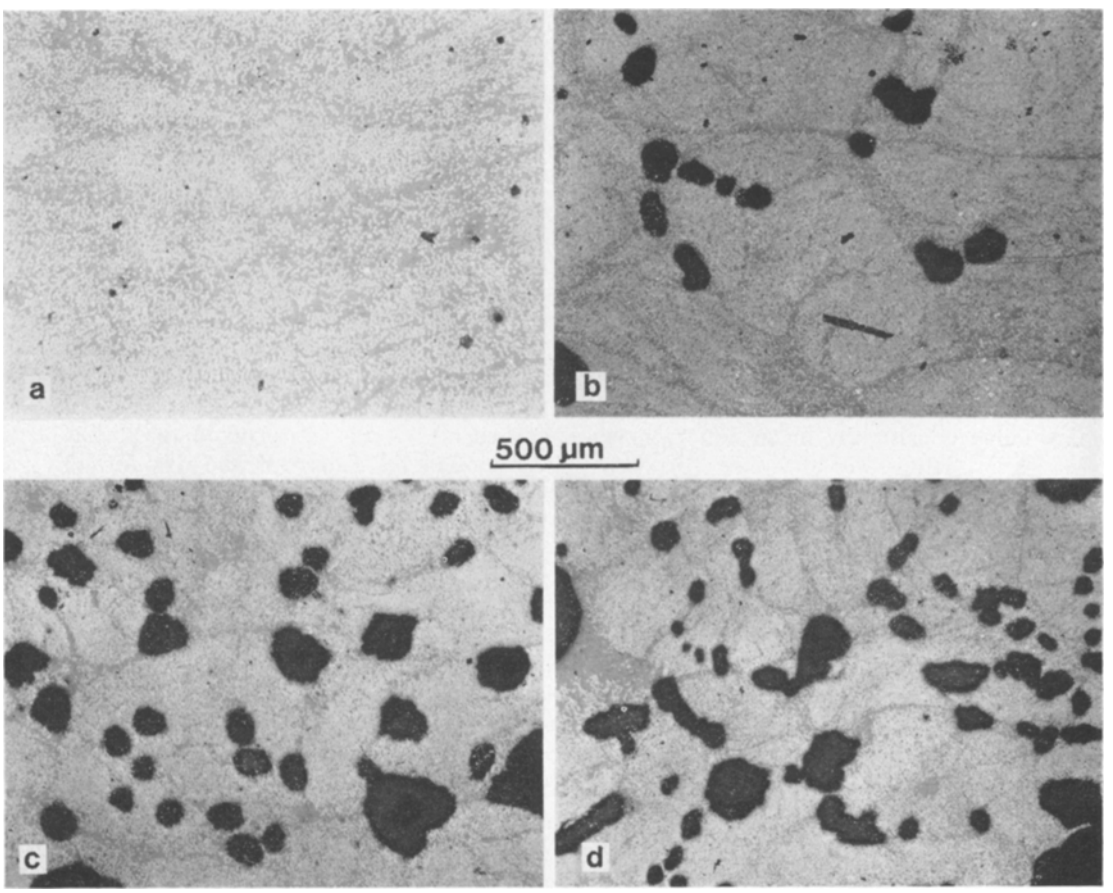

Figure 2 Microstructures of untreated fibre composites showing size, shape and distribution of voids: (a) zero voids; (b) 3% voids; (c) 8% voids; (d) 12% voids.

"pre-impregnation" method [11]. Aligned fibres are impregnated with a solution of epoxy resin in acetone in the ratio 2:1 by volume. The impregnated fibre mat contains approximately 55 wt % of resin and is dried in air at room temperature to remove the acetone. By varying the length of drying time, it is possible to control the amount of retained acetone in the fibre mat, and when the laminate is hot-pressed any residual acetone evaporates and is trapped in voids in the final composite. In the composites investigated the void content was deliberately varied between zero and 12%. The size, shape and distribution of these voids in the untreated fibre composite is shown in Fig. 2.

The resin system was "Epikote" 828/DDM pre-condensate and "Epikure" $BF_3$400 compounded in the ratio 125:4 parts by weight. The diameter of the carbon fibre was 7.93 ($\pm$ 0.61) $\times$ 10^{-6} m: its tensile strength was 1.58 ($\pm$ 0.44) GN m^{-2} and its Young's modulus was 360 ($\pm$ 31) GN m^{-2} (figures in parenthesis are standard deviations). The composites contained 40 vol % of either untreated or commercially surface treated fibres. The commercial treatment was the standard hypochlorite oxidation procedure.

3.2. Specimen design and mechanical testing

Simple flexural and interlaminar shear strength properties were measured on beam samples loaded in three-point bending using span:depth ratios of 25:1 and 5:1, respectively. The modes of failure in these two tests were always tensile and shear, except in surface treated fibre composites which failed consistently in tension even when using a span:depth ratio of 5:1.

Two types of fracture processes have been investigated; (1) where the crack has propagated in a direction perpendicular to fibres, and (2) where the crack extended parallel with the fibres.

3.2.1. Crack propagation perpendicular to fibres

The work to fracture the composites has been measured by three independent methods. Two of these involve determining the energy necessary to create two new fracture surfaces during total separation of the composite in bending. This energy includes that dissipated in the initiation of a failure crack and the work to propagate a moving crack through the material, and this can be defined as the work of fracture of the composite, γ_F. The third method involved fracturing a centre-cracked plate in tension to obtain the energy-release rate, γ_I, at the initiation of composite fracture. K_{Ic} was calculated from the maximum gross stress for unstable crack growth using an analysis by Isida [12] and γ_I obtained using Equation 4.

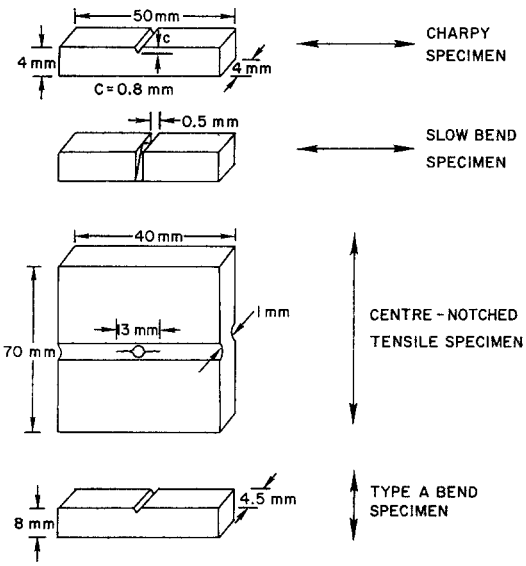

Figure 3 Design of specimens used for fracture energy measurements.

The work of fracture, γ_F, was measured at two different strain rates, using a slow three-point bend test and a four-point Charpy impact test. The slow bend test was carried out at a crosshead speed of 2×10^{-5} m sec^{-1} on specimens of the type used by Tattersall and Tappin [13]. The work of fracture is obtained from the integrated load/deflection curve divided by twice the nominal surface area.

Impact tests were carried out on a miniature Charpy machine of 2.75 Joules capacity and striker velocity 2.54 m sec^{-1} on single edge-notched square bars, in which the root of the notch had been sharpened with a scalpel blade. The energy absorbed by the pendulum during complete fracture of the sample is read directly from the machine and is divided by twice the fracture area to obtain γ_F. In both of these tests, γ_F is essentially the energy required to propagate a dynamic crack through unit area of composite material. The design of the specimens is shown in Fig. 3.

3.2.2. Crack propagation parallel to fibres

Rectangular section bars containing fibres in the direction perpendicular to the long axis were fractured in slow three-point bending. In some of the tests, specimens were positioned so that the span:depth ratio was 4:1 (type A specimens). By turning the bars through 90° the span:depth ratio could be changed to 8:1 (type B specimens). Several type A specimens were edge-notched using a 0.2 mm thickness cutting wheel and from the critical load to initiate cracking, K_{Ic} was determined using an analysis by Gross and Srawley [14]. Since the reinforcing effect of the fibres was small the flexural transverse modulus of the composite was used as a first approximation in Equation 3 to obtain γ_I. The specimen design is again shown in Fig. 3.

3.3. Fracture energy of epoxy resin

Triangular and single edge-notched beam specimens were machined from "as-cast" epoxy resin and exposed to the same conditions as the composite materials. Fracture was carried out in slow three-point bending and Charpy impact. The value of γ_I was calculated from a measurement of K_{Ic} and Equation 3 and γ_F was obtained from the area-under-curve method and from the Charpy energy.

4. Results

4.1. Effect of porosity on strength

The presence of voids in the resin phase and at the fibre/resin interface has a strong effect on the flexural strength and stiffness of the composite (Fig. 4). This is perhaps not surprising if we recall that a void content of 10% in a 40 vol% fibre composite implies a porosity of about 20% in the resin. Several models have been proposed to explain the effect of porosity on the strength and stiffness of composites [15-18]. Except for the analysis of Foye [17], all of these approaches assume that the composite contains a random dispersion of spherical voids. Foye's work indicated that cylindrical voids may have a more severe effect than spherical ones. The analysis of Rosen [19] predicts that the longitudinal tensile strength of the composite obeys a linear relationship between strength and volume fraction of fibre, and a non-linear variation with shear modulus of matrix (G_m). The observed decrease in flexural strength was, therefore, affected by voids only inasmuch as the matrix stiffness was affected by the porosity.

In considering the effect of porosity on the

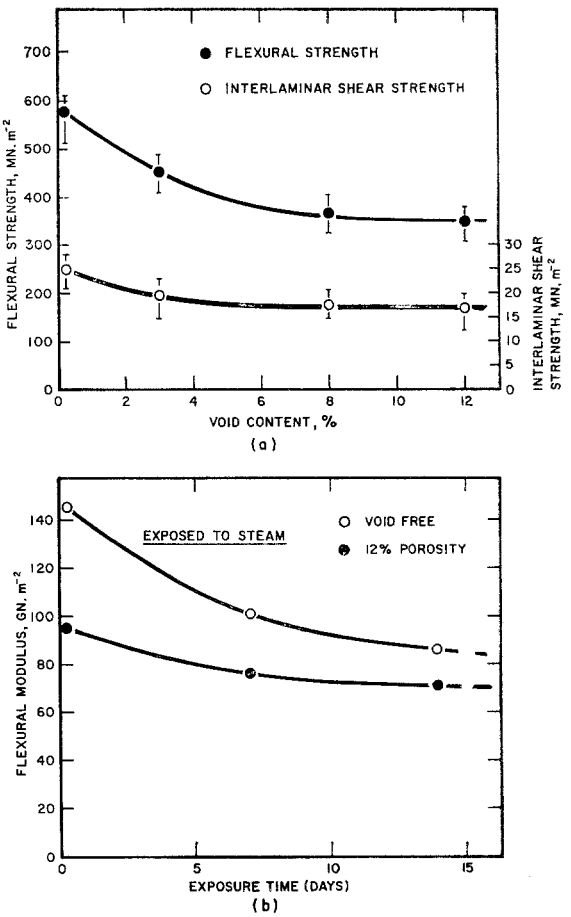

Figure 4 Effect of voids on the strength and stiffness of untreated fibre composites: (a) flexural strength and interlaminar shear strength versus void content; (b) effect of steam at 100°C on flexural modulus.

interlaminar shear strength of the composite, we shall examine two different cases of void shape and distribution, namely, spherical pores with cubic array, and cylindrical holes in a rectangular array.

First we consider the effects of voids on the shear strength of the resin and relate the results to the interlaminar shear strength of the composite. If the resin is assumed to contain spherical voids and is subjected to an average shear stress, τ_c, then the maximum shear stress will occur where the peripheries of adjacent voids are closest. If stress concentration effects are neglected, the maximum stress, $\tau_{c(max)}$, for the resin only is [15];

$$\tau_{c(max)} = \frac{\tau_c}{1 - \frac{\pi}{4}\left(\frac{6\epsilon}{\pi}\right)^{2/3}}$$

where

$$\epsilon = \frac{V_v}{V_v + V_m} - \frac{\pi}{6}\left(\frac{R}{l_s}\right)^3$$

R being the radius of the void and l_s half the distance between centres of the spherical voids. V_v and V_m are the volume fraction of voids and matrix, respectively.

For a fibre composite containing voids,

$$\epsilon = \frac{V_v}{1 - V_f^*}$$

where V_f^* is the true fibre volume fraction of the composite.

The interlaminar shear strength of the composite is obtained by letting $\tau_{c(max)}$ be equal to the allowable shear strength of the void-free material, and solving for the average shear stress;

$$\frac{\tau_c}{\tau_{c\,(max)}} = 1 - \frac{\pi}{4}\left[\frac{6}{\pi}\left(\frac{V_v}{1 - V_f^*}\right)\right]^{2/3} \quad (6)$$

If the composite is assumed to contain cylindrical voids, however, the maximum shear stress will be;

$$\tau_{c(max)} = \frac{\tau_c}{1 - \left(\frac{4\epsilon}{\pi}\right)^{1/2}}$$

where

$$\epsilon = \frac{\pi}{4}\frac{R^2}{l_s} = \frac{V_v}{(1 - V_f^*)}$$

If the composite contains cylindrical holes, the relationship between τ_c, $\tau_{c(max)}$ and V_v is;

$$\frac{\tau_c}{\tau_{c(max)}} = 1 - \left(\frac{4V_v}{\pi(1 - V_f^*)}\right)^{1/2} \quad (7)$$

Fig. 5 shows a comparison between this theoretical approach and the experimentally measured values. The theoretical analysis for spherical voids shows a better correlation with the experimental $\tau_{c(max)}$ values for the porous material tested in air and after exposing to steam, but actual strengths are higher than predicted ones, perhaps because the void distribution is not random, as assumed in the models.

4.2. Effect of moisture on strength

A number of composite samples of varying void content was exposed to water at room temperature, steam at 100°C, and a mineral oil at 100°C for up to two weeks duration. The composites picked up only about 0.5 wt % of moisture during

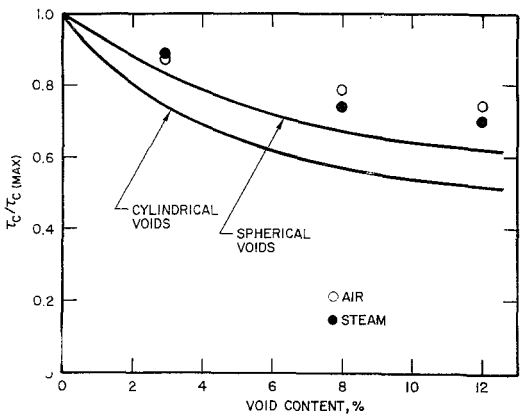

Figure 5 Comparison between theoretical and experimental values of interlaminar shear strength for void-free and porous untreated fibre composites.

immersion in water at ambient temperatures and their weight remained unaltered throughout exposure to oil at the elevated temperature. By contrast, as Fig. 6 shows, there was a continuous change in weight of the void-free material during

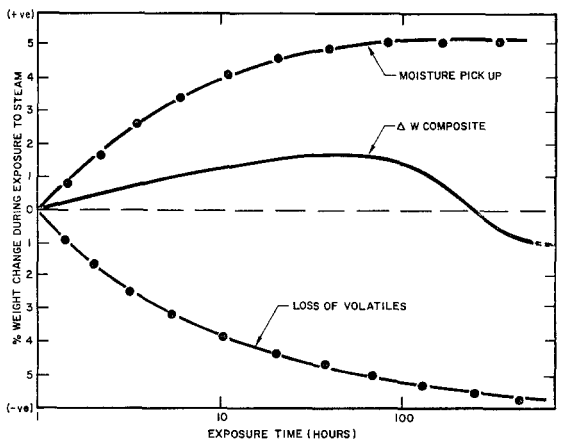

Figure 6 Amount of water absorption by untreated fibre composites during exposure to steam at 100°C.

exposure to steam. There is an increase in weight up to about 5% due to water absorption but at the same time a loss of volatile constituents from the epoxy resin. By weighing the unexposed composite, reweighing after exposure, and reweighing yet again after heating the material to rid it of moisture, it was possible to plot a curve of water pick-up and a curve for loss of volatiles (Fig. 6). A pure resin control sample picked up less than 0.1% moisture during similar periods of exposure. In an experiment where an untreated

fibre composite sample was boiled in water containing a fluorescent dye and then fractured so as to produce the characteristic fibrous appearance, it was possible under ultra-violet light to observe fluorescence on the surfaces of pulled-out fibres. This simple experiment suggests that much of the moisture is absorbed by capillary action at the fibre/resin interface. An accompanying increase of about 5% in composite volume suggests that the presence of moisture may have caused some swelling in the resin which could have resulted in a reduction of the residual compressive forces in the matrix over the surface of the fibres [20]. These compressive forces may even have been reversed leaving a resultant transverse tensile failure of the fibre-resin bond before any application of external applied stress.

Exposure of the untreated fibre composite to steam has resulted in a decrease in flexural modulus by about one-third (Fig. 4). For the material containing about 12% voids, the presence of moisture had only a marginal effect on the modulus of the composite. The effect of moisture on flexural strength and interlaminar shear strength of the untreated fibre composite is shown in Fig. 7. Water at ambient temperature has had little effect on these properties but exposure to steam has reduced both strengths by some 50%. The presence of more than about 2% voids has encouraged the ingress of moisture and the strength of the fibre-resin bond has suffered accordingly (Fig. 5).

The flexural strength of the surface-treated fibre composites was 0.60 GN m^{-2}. No shear failure could be induced in this material in short beam bending, but a *minimum* value of 50 MN m^{-2} for the interlaminar shear strength was estimated. Neither the flexural strength nor the interlaminar shear strength values were significantly affected by exposure of the strongly-bonded material to steam or oil, but the fracture

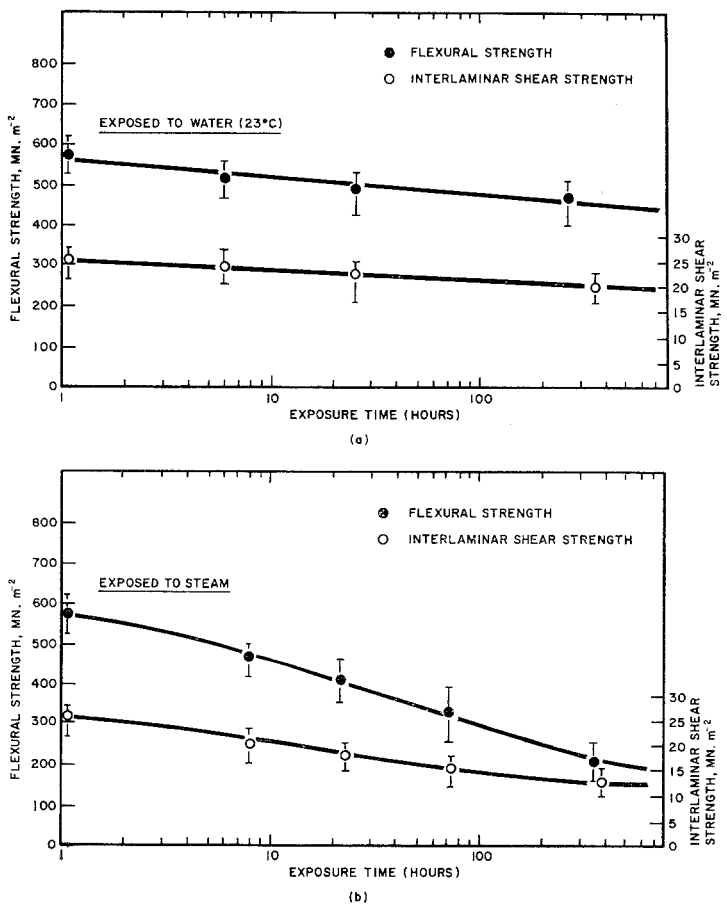

Figure 7 Effect of environment on flexural and interlaminar shear strengths of untreated fibre composites: (a) exposed to water at 23°C; (b) exposed to steam at 100°C.

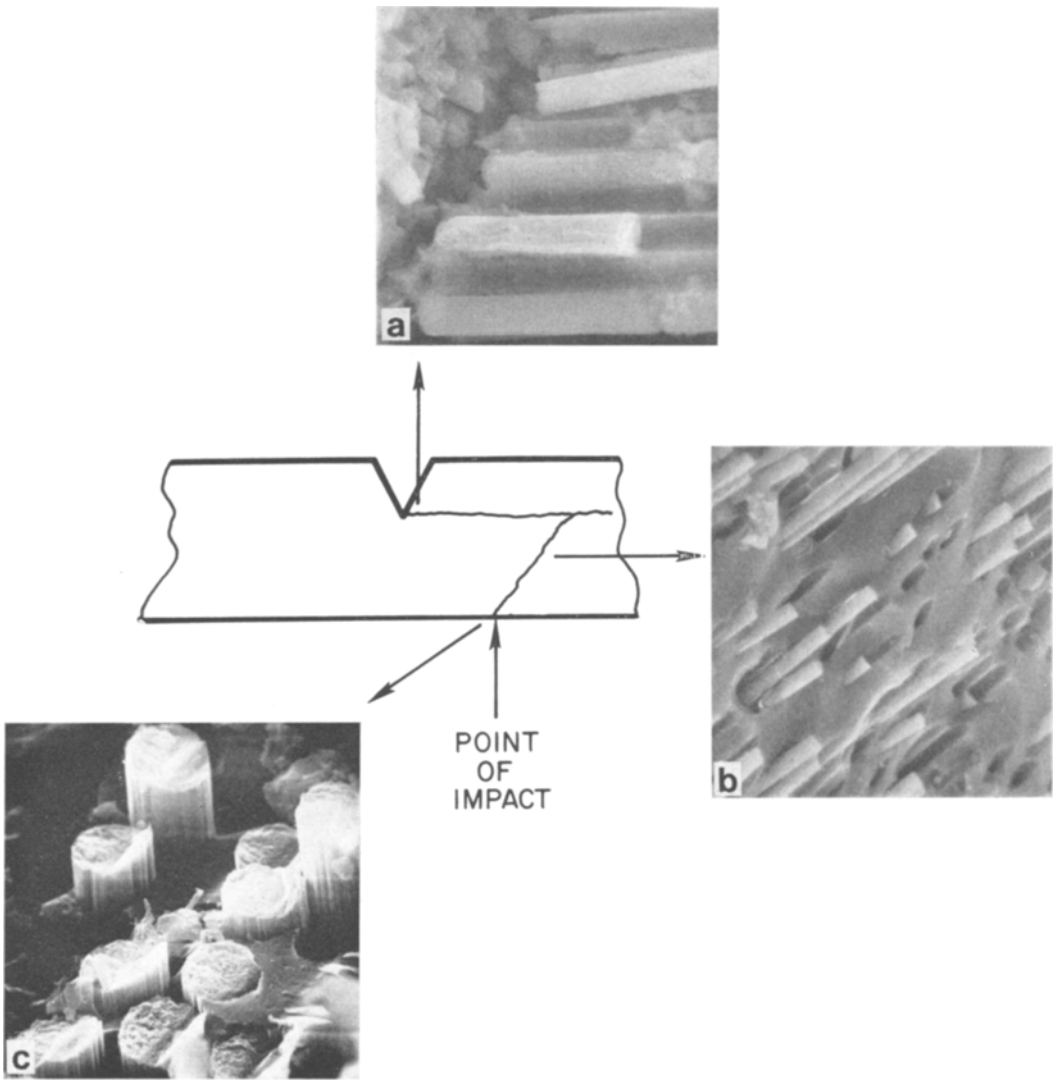

Figure 8 Some scanning electron microscope observations of the fracture surface of an untreated fibre composite after Charpy impact: (a) shear failure at tip of notch; (b) oblique fracture surface at 45° to fibre direction; (c) compression failures at point of impact.

strength of the notched composite was reduced by one-third.

4.3. Fracture perpendicular to fibres

Under certain conditions, the energy required to break a composite in a controlled bend test may be considered equivalent to the energy absorbed by the pendulum during impact fracture and equated to the energy released during propagation of a moving crack. However, the modes of failure in the two tests were quite different. Fracture of the triangular section specimens occurred by the initiation and propagation of a planar tensile crack accompanied by the pulling out of broken fibres behind the advancing crack front. By contrast, fracture under impact loading

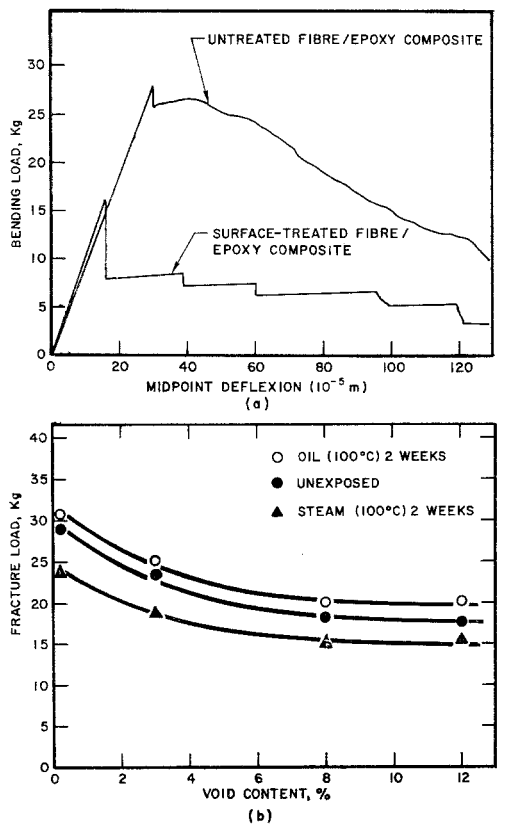

Figure 9 (a) Typical load/deflection curves obtained during slow bending of triangular-section specimens; (b) effect of void content on ultimate fracture load of triangular-section specimens during slow bend testing.

was complex and consisted of a mixture of tensile, shear and compression failure modes (Fig. 8). Typical load/deflection curves for the triangular section specimens are shown in Fig. 9. The behaviour of the two types of material is quite different.

Microscope examination of the fracture surface of untreated fibre composite at the apex of the triangle shows a planar matrix surface with protruding fibres extending to an average length of about 3 fibre diameters, at least an order of magnitude less than that observed in the bulk of the material (Fig. 10). The short pull-out lengths may be associated with the rapid extension and opening of the matrix crack, with a corresponding high rate of fibre extraction [21]. If the epoxy resin is capable of viscoelastic behaviour, the shear stresses along the interface may relax as a consequence of the time-dependent properties of the matrix, and the critical fibre transfer length, l_c, will, in turn, be a rate-dependent parameter [22, 23]. Composites exposed to steam did not show this rapid fall off in load at the initiation of fracture, but failure was controlled and the length of pulled out fibres was reasonably constant over the whole fracture surface (Fig. 10).

4.3.1. Energy released during crack initiation

Values of K_{Ic} and γ_I obtained experimentally by fracturing centre-notched plates perpendicular to the direction of fibres are presented in Table II. The values of γ_I are similar to the values of γ_F measured by Charpy impact and slightly above the values determined from slow bending shown alongside. Clearly, the effect of improving the strength of the fibre-resin bond has been at the expense of the composite's resistance to the propagation of static cracks and γ_I has been reduced by a factor of about 5. Exposure to steam had little effect on γ_I for the untreated fibre material but reduced γ_I for the strongly-bonded composite by a factor of about 2. The experimental values of γ_I are much greater than the theoretical estimates of γ_d or γ_r but are in good agreement with γ_p (see Section 5). The values of γ_I were unaltered after exposure of the composites to oil at 100°C for up to two weeks although the fracture load of the triangular-section specimens had increased slightly (Fig. 9).

4.3.2. Energy released during crack propagation

Fig. 11 shows the influence of voids on the work of fracture of untreated fibre composites measured in slow bending and Charpy impact. In these tests, the Charpy impact values were consistently higher than the slow-bend values. Only when the strength and stiffness of the composite had been reduced by the porosity or by exposing the material to steam did the two tests give similar results (Fig. 12). Where the strength and stiffness had been reduced significantly for the porous composite containing 12% voids, the γ_F values measured by the two tests were virtually indistinguishable. γ_F measured in slow bending was not significantly changed by exposing to steam, although the average fibre pull-out length in the weakly-bonded material increased by about a factor of 2 (Fig. 10).

The effect of surface treating the fibres was to decrease both the average fibre pull-out length (Fig. 10) and the resistance of the composite to propagating cracks, γ_F, by nearly an order of magnitude.

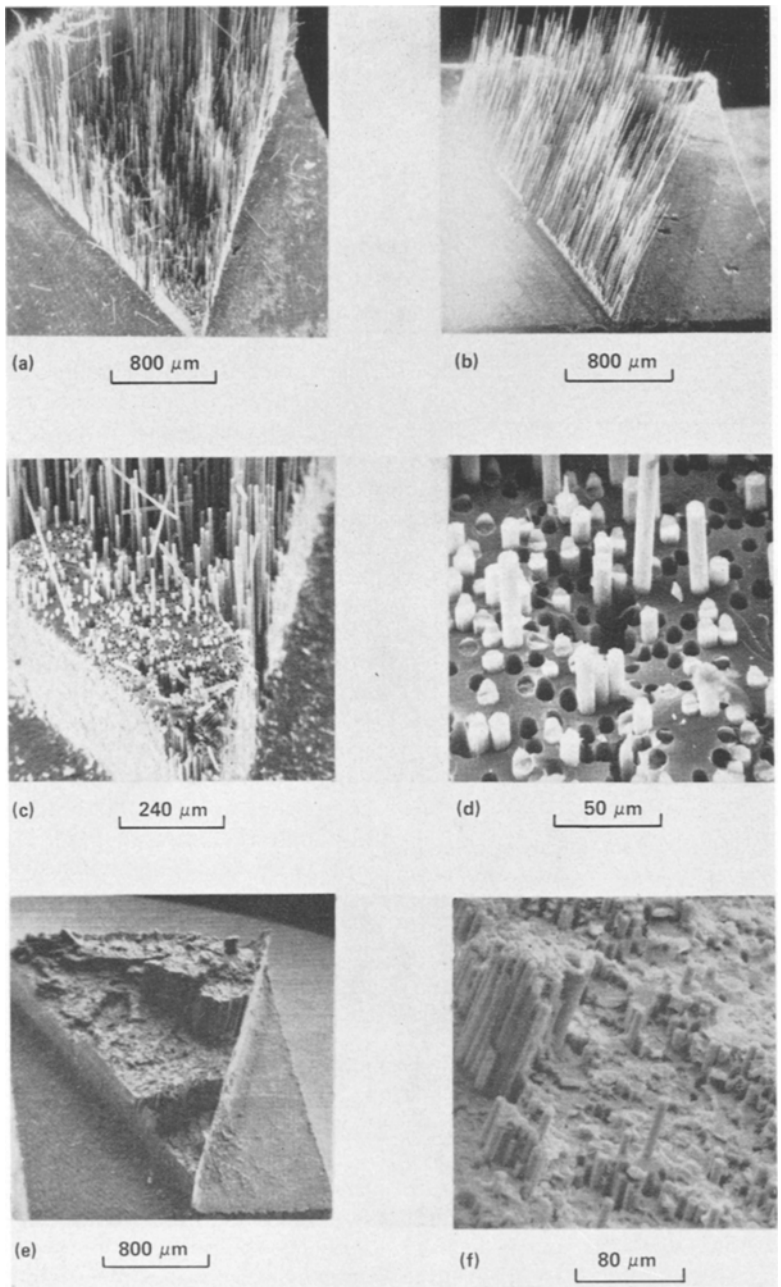

Figure 10 Fracture surfaces of untreated and treated fibre composites observed in the scanning electron microscope: (a) untreated fibre composite; (b) similar to (a) but after exposure to steam; (c) and (d) high magnification of (a) at apex of the triangle; (e) and (f) treated fibre composite.

4.4. Crack propagation parallel with fibres

Table III shows experimental values of K_{Ic}, γ_I and γ_F obtained for the unreinforced epoxy resin and fibre composites. In spite of the difference in bond strength between the untreated and surface-treated fibre composites, the energies required to initiate and propagate a crack in the direction of fibres are similar and not unlike the fracture surface energy of the epoxy resin.

The most obvious difference between the two

TABLE II Fracture toughness and work of fracture for cracking normal to fibres

Material	Environment	Tensile test		Charpy test	Slow bend test	$\gamma_p = \frac{V_f \tau_i' l_c^2}{12 d}$
		K_{Ic} (MN m$^{-3/2}$)	γ_I (kJ m^{-2})	γ_F (kJ m^{-2})	γ_F (kJ m^{-2})	(kJ m^{-2})
Untreated carbon/epoxy	Air	41.5	33.0	35.0	23.0	26.0
	Steam	43.5	36.5	30.0	20.0	
Treated carbon/epoxy	Air	18.7	7.0	9.0	2.5	2.5
	Steam	13.0	3.4	5.2	2.1	

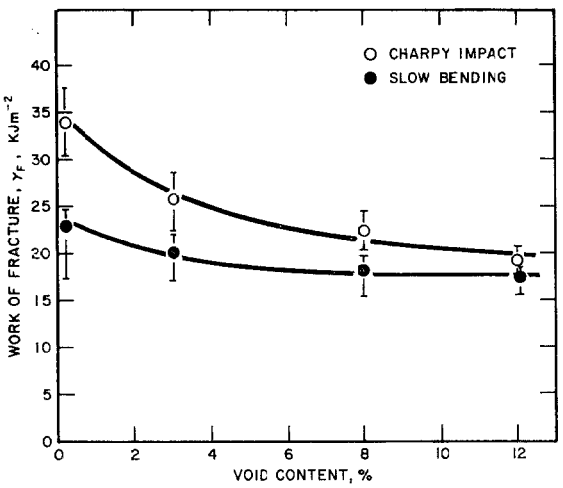

Figure 11 Effect of void content on the work of fracture of untreated fibre composites perpendicular to fibres.

composites is their apparent resistance to degradation by exposing to steam gauged by the decrease in K_{Ic} and γ_I of the weakly-bonded material. Under such conditions, crack initiation is being influenced by the weakened fibre/resin interface but the high γ_F values indicate that the

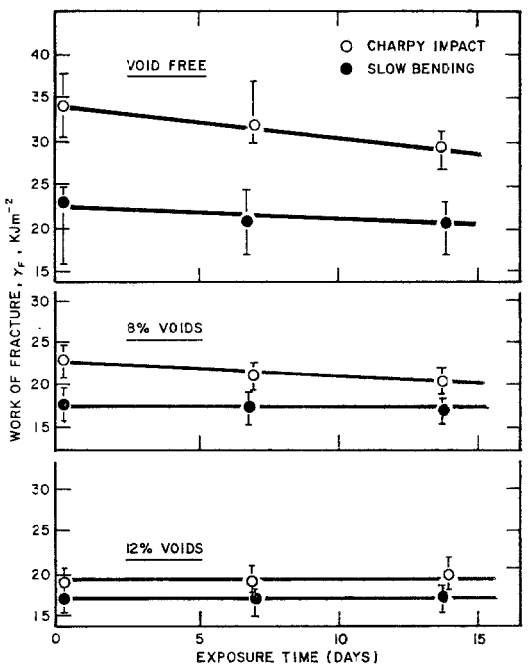

Figure 12 Effect of exposure to steam at 100°C on the work of fracture of untreated fibre composites perpendicular to fibres.

TABLE III Fracture toughness and work of fracture parallel to fibres

Material	Environment	Interlaminar shear strength (MN m^{-2})	K_{Ic} (MN m$^{-3/2}$)	γ_I (J m^{-2})	γ_F (J m^{-2})
828/DDM epoxy resin	Air		1.20	345	330
	Steam		1.05	250	144
	Oil		1.04	260	190
Untreated carbon/epoxy	Air	25	1.1	255	263
	Steam	16	0.6	75	235
	Oil	22	1.0	240	330
Treated carbon/epoxy	Air	> 50	1.2	340	208
	Steam		1.1	290	229
	Oil		1.2	340	233

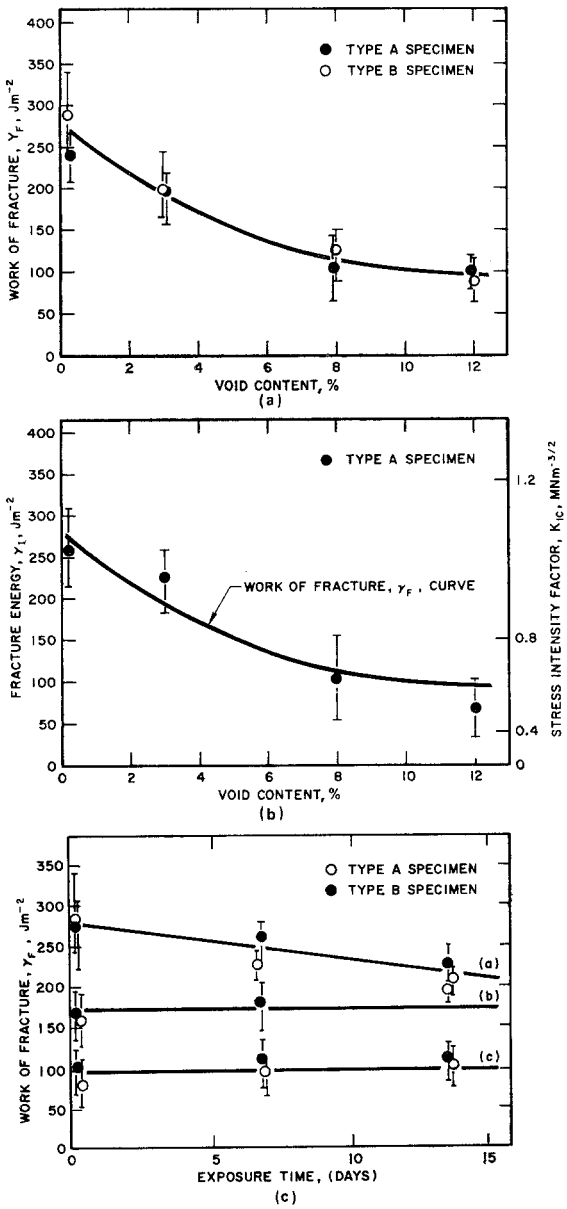

Figure 13 Fracture energy measurements on untreated fibre composites parallel to fibres: (a) effect of void content; (b) comparison between γ_F and γ_I values; (c effect of exposure to steam at 100° C (a zero voids, b 3% voids, c 12% voids).

matrix is controlling the growth of the crack as fracture proceeds.

There is no appreciable difference between γ_F values measured using types A and B specimens (Fig. 13), and there is good agreement between the values of γ_F and γ_I for the unexposed material. The effect of a few per cent voids has reduced both of these by similar amounts. Exposure to steam has reduced γ_F slightly for the void-free material only.

5. Discussion

5.1. Energies to propagate a crack perpendicular to fibres

If the release of energy at the initiation of failure can be equated to the loss of stored elastic strain energy in a fibre when it debonds and snaps, then the fracture surface energy of the composite according to Outwater and Murphy [5] is:

$$\gamma_I \equiv \gamma_d = \frac{V_f \sigma_f^2 y}{4E_f} \tag{8}$$

where V_f is the volume fraction of fibres and y is the length of fibre over which debonding has taken place. This assumes that the interfacial shear strength of the fibre-matrix interface is zero after debonding and therefore the release of stored energy is irreversible. However, if the shear stress at the interface is maintained *after* the fibre snaps, then the loss of energy when the fibre relaxes is [4]:

$$\gamma_I \equiv \gamma_r = \frac{V_f \sigma_f^2 l_c}{6E_f} \tag{9}$$

This can be re-written in terms of the fibre diameter, d, and the interfacial shear stress, τ_i, using the relationship [24];

$$\frac{l_c}{d} = \frac{\sigma_f}{2\tau_i} \tag{10}$$

where l_c is the minimum length of fibre surrounded by a matrix which can be loaded to its breaking stress. We then have;

$$\gamma_r = \frac{V_f \sigma_f^3 d}{12E_f \tau_i} \tag{11}$$

From Equation 11 it can be seen that γ_r is inversely proportional to τ_i, and comparing Equations 8 and 9, $\gamma_d > \gamma_r$. Rough estimates of γ_d and γ_r suggest that these are insignificant compared with the measured composite fracture energies. They are in fact of the order of only 0.5 kJ m^{-2} for the untreated fibre composites and about a tenth of this for the treated fibre material.

5.2. Crack propagation and fibre pull-out

When a fibre snaps, the interfacial shear stress, τ_i, may fall to some finite value, τ_i', the frictional interfacial shear stress. Behind the crack front, a certain number of broken fibres will pull out of the matrix, and the frictional forces acting along

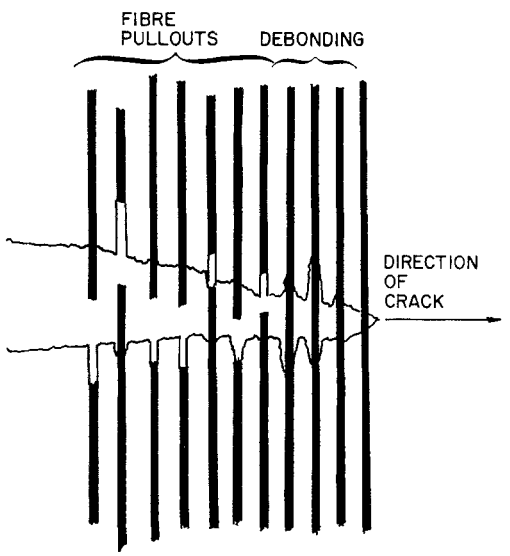

Figure 14 Schematic representation of the propagation of a microcrack perpendicular to fibres showing debonding at the crack tip and fibres pulling out behind the advancing crack front.

the fibre/resin interface will resist the opening and extension of the matrix crack (Fig. 14). It can be shown that the energy required to overcome the restraining forces at the interface and to pull out discontinuous fibres of length l_c, is given by [6]:

$$\gamma_p = \frac{V_f \sigma_f l_c}{24} \tag{12}$$

$$= \frac{V_f \tau_i' l_c^2}{12d} \tag{12a}$$

The average length of protruding carbon fibre can be considered as equivalent to $l_c/4$ and γ_p can, in principle, be computed from the above equation. In our experiments we have varied the shear strength of the fibre/resin interface, τ_i, by an order of magnitude, and from Equation 10 we can estimate the value of l_c for the different composites. Theoretical γ_p values can now be predicted for this kind of material having a range of values of frictional shear stress, τ_i', from zero up to the shear strength of the resin matrix (Fig. 15). Superimposed on this theoretical plot are experimental values of γ_F for the untreated and commercially surface treated fibre composites, together with other work of fracture data of CFRP composites containing fibres surface treated by other methods [25, 3].

From scanning electron microscope studies of the fracture surfaces of carbon fibre-reinforced resin systems, the average fibre pull-out lengths for the untreated and commercially-treated fibre composites are about $30d$ and 2 or $3d$, respectively (Fig. 10). Substituting values for fibre strength, fibre diameter, and the critical fibre transfer length, l_c (obtained from pull-out measurements) into Equation 10, the interfacial shear stress, τ_i, for the untreated fibre composite is about 6.7 MN m^{-2} while that for the commercially-treated fibre composite is 80 MN m^{-2}.

An approximate measurement of the interfacial shear strength can be obtained indirectly from the short beam flexural results using an approach of Hancock and Cuthbertson [26] where:

$$\tau_i = \frac{\tau_c - (1 - x)\tau_m}{x} \tag{13}$$

τ_i is the interfacial shear strength; τ_c is the measured interlaminar shear strength; and τ_m, is the shear strength of the resin.

The fraction, x, of fracture surface area of fibre/resin interface to the total surface area of one of the shear fracture planes is given by:

$$x = \frac{(V_f \pi)^{1/2}}{(V_f \pi)^{1/2} + 1 - 2(V_f/\pi)^{1/2}}$$

V_f, the volume fraction of fibre is simply;

$$V_f = \left(\frac{\pi d^2}{4}\right)\frac{1}{b^2}$$

where b is the distance between centres of two adjacent fibres.

For the untreated fibre composite, substituting the values 0.40, 0.80, 25 MN m^{-2} and 90 MN m^{-2} for V_f, x, τ_c and τ_m, into Equation 13, τ_i will be approximately 6.3 MN m^{-2}, in good agreement with the value of τ_i just estimated from fibre pull-out measurements. The value of τ_i is about one-quarter of the experimental value of interlaminar shear strength, τ_c, of the composite.

The mean observed length of protruding fibre was about $30d$ for the untreated fibre composites and if we assume that the interfacial shear stress is similar to the frictional shear stress at the interface during fibre pull-out, then from Equation 12 $\gamma_p = 26$ kJ m^{-2}.

Similarly, the work required to extract commercially treated fibres from the cracked resin matrix, where l_c is about $10d$ and τ_i is about 80 MN m^{-2} is given by Equation 12a as $\gamma_p = 2.2$ kJ m^{-2}.

We assume that the value of τ_i and τ_i' for these composites are approximately equal. It can

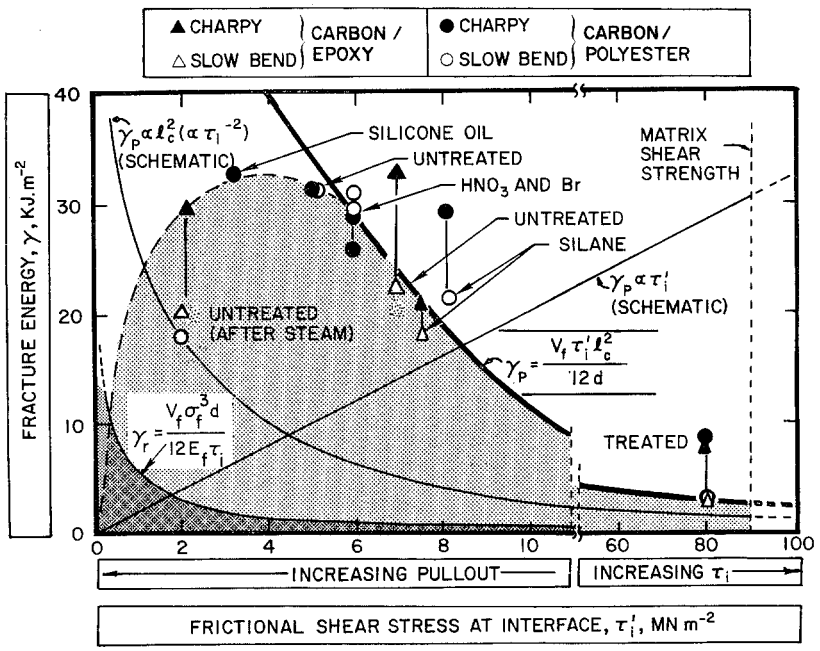

Figure 15 A theoretical plot of fracture energy with variation of frictional interfacial shear stress, τ_i' compared with experimental work of fracture values. For details of polyester/carbon fibre data refer to ref. [3].

be seen that the values of γ_F obtained by integration of the load-deflection curve are in good agreement with the values of γ_p obtained using this theoretical approach (Fig. 15). We conclude that the pull-out energy, γ_p, consumed during the opening and extension of the resin crack contributes primarily to the work to propagate a dynamic crack in a controlled manner through these composites.

Exposure of the untreated fibre composite to steam resulted in an increase of l_c by at least a factor of two, to a value of about $200d$ (Fig. 10). The effect of moisture was to reduce the compressive forces of the resin over the surface of the fibres so as to encourage debonding at the fibre/resin interface. The debonded length will depend on the value of τ_i. Substituting a value of l_c of $200d$ into Equation 10, τ_i is calculated to be close to 4 MN m^{-2}. Now the measured value of work of fracture, γ_F, in slow bending, was about 23 kJ m^{-2} which is derived primarily from γ_p. If the measured value of γ_F and estimated value of l_c are inserted into Equation 12a, the value of τ_i' comes out close to 2 MN m^{-2}, which is about half τ_i, probably because of the presence of a lubricating moisture film at the interface.

The apparent fracture toughness, K_{Ic}, measured for the *untreated fibre composite* fractured in air was about 40 MN m$^{-3/2}$. Substituting into Equation 4 together with the estimated value of $E_{(effective)}$ we have:

$$G_{Ic}/2 \equiv \gamma_I = 21 \text{ kJ m}^{-2}$$

Similarly, the fracture toughness, K_{Ic}, of the *treated fibre composite* was about 18 MN m$^{-3/2}$, so that $\gamma_I = 4.25$ kJ m^{-2}. After exposing the treated fibre composite to steam, K_{Ic} decreased to a value of 13 MN m$^{-3/2}$ and γ_I is therefore 2.2 kJ m^{-2}.

The effect of moisture was to reduce the energy to *initiate* unstable fracture of the well-bonded material by about one-half. All the γ_I values are similar to the γ_F values measured in slow bending. For the untreated fibre composite, perhaps this could be considered fortuitous in view of some work of Beaumont and Phillips [27] who have shown that the application of linear elastic fracture mechanics to *weakly-bonded* composites may be invalid.

Improving the interfacial shear strength of the composite by about an order of magnitude has resulted in a drastic reduction of γ_I. It appears that the energies necessary to propagate a static crack and a moving crack under controlled conditions are very similar. For the treated fibre composite exposed to steam, the reduction in γ_I by about a factor of 2 can be accounted for by

the decreased notched strength of the material. This would also account for the reduction in Charpy impact energy after exposure to moisture.

6. Conclusions

These results suggest that the energies dissipated in crack initiation and propagation in the weakly-bonded composite are derived principally from the work of fibre pull-out, γ_p, but in the strongly-bonded material the Griffith fracture energy, γ_I, is greater than γ_p and is determined mainly by the amount of work to fracture a brittle orthotropic solid.

The simple approach of equating the work of fracture, γ_F measured in slow bending with theoretical values of γ_p calculated using Equation 12a is apparently an acceptable approximation, as shown in Fig. 15. It is postulated that the energy required to propagate a slowly moving crack in CFRP composites is proportional to l_c^2 and τ_i', the frictional interface shear stress, and the increase in one of these parameters is at the expense of the other. The poor correlation between the work of pull-out and the total work of fracture for the untreated fibre composites exposed to steam is because τ_i' becomes significantly less than τ_i, the total interface shear stress. The fibre pull-out length is controlled by the value of τ_i and the theoretical value of γ_p is determined by τ_i'. The good agreement between γ_F and γ_p above a minimum τ_i' value is an indication of the similarity between τ_i and τ_i' during pulling out of the broken fibres.

Acknowledgements

The work described here is part of a research programme on the mechanical and fracture behaviour of CFRP funded by the Science Research Council, Imperial Chemical Industries, and Guest, Keen and Nettlefolds Limited, and we gratefully acknowledge their support. One of us (P.W.R.B.) was supported by an SRC studentship at the time the work was carried out. We thank Dr D. C. Phillips and Mr C. D. Ellis for several helpful discussions on this work.

References

1. A. A. GRIFFITH, *Phil. Trans. Roy. Soc.* **A221** (1921) 163.
2. P. W. R. BEAUMONT and D. C. PHILLIPS, *J. Mater. Sci.* **7** (1972) 682.
3. B. HARRIS, P. W. R. BEAUMONT, and E. MONCUNILL DE FERRAN, *ibid* **6** (1971) 238.
4. J. FITZRANDOLPH, D. C. PHILLIPS, P. W. R. BEAUMONT, and A. S. TETELMAN, *ibid* **7** (1972) 289.
5. J. O. OUTWATER and M. C. MURPHY, 24th Annual Conference of Reinforced Plastics/Composites Division of Soc. Plastics Ind., paper 11-C (1969).
6. A. H. COTTRELL, *Proc. Roy. Soc.* **A282** (1964) 2.
7. G. C. SIH, P. C. PARIS, and G. R. IRWIN, *Internat. J. Fracture Mech.* **1** (1965) 189.
8. E. M. WU, *J. Applied Mech. Trans. ASME*, Series E, **34** (1967) 967.
9. G. R. IRWIN, "Handbuch der Physik", **6** (Springer-Verlag, Berlin, 1958) 551.
10. S. W. TSAI, "Formulas for the Elastic Properties of Fiber Reinforced Composites", Monsanto/Washington University ONR/ARPA Association, HPC 68-61 (1968).
11. P. W. R. BEAUMONT, "Fracture and Fatigue of Carbon Fibre Reinforced Plastics", D.Phil. Thesis, School of Applied Sciences, University of Sussex (1971).
12. M. ISIDA, unpublished data described by W. F. Brown and J. E. Srawley, "Plane Strain Crack Toughness Testing of High Strength Metallic Materials", ASTM, STP 410, 1966 p. 11.
13. H. G. TATTERSALL and G. TAPPIN, *J. Mater. Sci.* **1** (1966) 296.
14. B. GROSS and J. E. SRAWLEY, Technical Note D-3092, NASA, December, 1965. (Described in ASTM STP 410 p. 13.)
15. L. B. GRESZCZUK, "Effect of Voids on Strength Properties of Filamentary Composites", Conference of Reinforced Plastics/Composites Division of SPI, 1967.
16. B. BUDIANSKY, *J. Mech. Phys. Solids* **13** (1965) 223.
17. R. L. FOYE, *AIAA* paper no. 66-143, (1966).
18. N. A. WEIL, "Parametric Effects on the Mechanics of Ceramic Materials", Symp. on Ceramic Materials (1966).
19. B. W. ROSEN, *AIAA J.* **2** (1964) 1985.
20. R. C. WYATT and K. H. G. ASHBEE, *Fibre Sci. and Tech.* **2** (1969) 29.
21. P. W. R. BEAUMONT and B. HARRIS, "Effect of the Fibre-Matrix Interface on the Fracture Toughness of Carbon Fibre Resin Composites", Fifth Symposium on Advanced Composites, St. Louis, Missouri, Washington University/Monsanto (April 1971).
22. R. G. C. ARRIDGE, *Nature* **223** (1969) 941.
23. J. M. LIFSHITZ and A. ROTEM, *Fibre Sci. and Tech.* **3** (1970) 1.
24. A. KELLY and G. J. DAVIES, *Met. Rev.* **10** (1965) 1.
25. B. HARRIS, P. W. R. BEAUMONT, and A. ROSEN, *J. Mater. Sci.* **4** (1969) 432.
26. P. HANCOCK and R. C. CUTHBERTSON, *ibid* **5** (1970) 762.
27. P. W. R. BEAUMONT and D. C. PHILLIPS, *J. Comp. Mater.* **6** (1972) 32.

Received 14 February and accepted 27 March 1972.